A Combined Experimental and Theoretical Study on the Conformational Behavior of a Calix[6]arene

Béatrice Boulet,[†,‡] Laurent Joubert,[†] Gérard Cote,[†] Céline Bouvier-Capely,[‡] Catherine Cossonnet,[‡] and Carlo Adamo*[,†]

Laboratoire d'Electrochimie et Chimie Analytique, UMR CNRS-ENSCP 7575, Ecole Nationale Supérieure de Chimie de Paris, 11 rue P. et M. Curie, F-75231 Paris Cedex 05, France, and IRSN/DRPH/SDI/LRC, BP 17, F-92262 Fontenay-aux-Roses CEDEX, France

Received: November 11, 2005; In Final Form: February 21, 2006

An experimental and theoretical study on the conformational behavior of the 1,3,5-OMe-2,4,6-$OCH_2CONHOH$-*p-tert*-butylcalix[6]arene has been carried out. In particular, semiempirical (AM1) and density functional theory (DFT) calculations have been performed in order to identify the possible conformers. The obtained results show that the cone structure is the most stable conformer at any level of theory, even if significant differences have been obtained for the other species. The inclusion of solvent effect, through a continuum model, also points out the relevant role played by the solvent in the stabilization of the cone structure in solution. These latter results have been confirmed by NMR experiments, which clearly show the presence of only the cone conformer in a polar solvent, such as DMSO. Finally, ^1H and ^{13}C NMR spectra on model systems, i.e., two successive phenol rings ($Ar_1-CH_2-Ar_2$), have been computed at the DFT level and compared with the experimental spectra of the complete molecule. The results show an overall good agreement with the experimental data, thus leading to an unambiguous assignment of the experimental spectra.

1. Introduction

Calixarenes have been extensively studied during the past decade, due to their versatility in terms of complexing capability, conformational flexibility, and reactivity. Such peculiar chemical characteristics have been exploited in a large variety of chemical applications, including catalysis, host−guest chemistry, separation chemistry, selective ion transport, and sensors.[1] Within these applications, these macrocyclic molecules are particularly interesting for their properties related to the actinide extraction.[2,3] In fact, they can selectively extract neutral or charged molecules, and such properties can be easily modified and tuned, since they depend on the size of the molecular cavity, the geometry of coordination, and the functionalization of lateral groups.[4] A large number of experimental studies on the complexation mechanism have been carried out in the past years.[3−8] Thus, calix[6]arenes bearing carboxylic, phosphonic, or hydroxamic acid groups have been widely studied as specific ligands for the uranyl ion (UO_2^{2+}).[9−17] More recently, it has been shown that calix[6]arenes bearing hydroxamic functions, such as the 1,3,5-OMe-2,4,6$OCH_2CONHOH$-*p-tert*-butylcalix[6]arene (Figure 1) are particularly suitable to complex selectively the uranyl ion.[11−13,18]

In an experimental context, the understanding of the conformation behavior of calixarenes is a necessary prerequisite to rationalize their properties and to drive future syntheses. Experimental studies showed that calix[*n*]arenes present a preorganized flexible structure in solution.[8] These macrocyclic molecules are composed of *n* phenolic units linked by methylene bridges at ortho positions, with various groups on the upper (the para position) and lower rims (phenolic OR groups).[19] Their flexibility is due to two possible rotational modes of the phenol units, the so-called "oxygen-through-the-annulus" (OTA) and the "para-substituent-through-the-annulus" (PSTA) rotations.[20] Experimental conformational features of calixarenes have been deeply analyzed by NMR spectroscopy, using ^1H, ^{13}C, time-scale dependence, NOESY, and ROESY techniques.[20−24] In particular, Van Duynhoven and co-workers studied the influence of lower rim alkyl substituents on the conformations of 1,3,5-OR_1-2,4,6-OR_2-*p-tert*-butylcalix[6]arenes.[23] They suggested that methyl or ethyl R_1 groups favor a highly symmetric (C_{3v}) cone

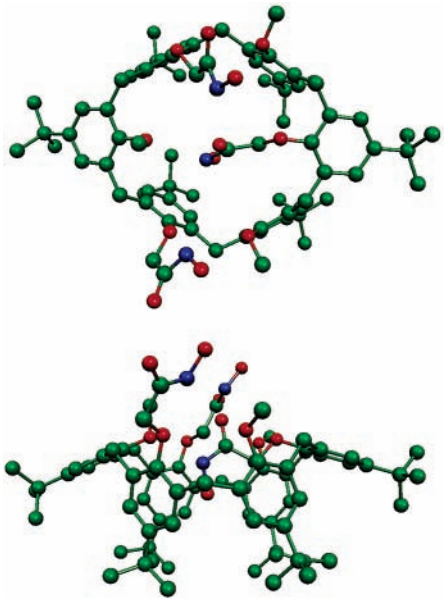

Figure 1. Structure of most stable conformer of 1,3,5-OMe-2,4,6-$OCH_2CONHOH$-*p-tert*-butylcalix[6]arene (cone conformation). Hydrogen atoms are omitted for clarity.

* Corresponding author: carlo-adamo@enscp.fr.
† ENSCP.
‡ IRSN.

10.1021/jp0565305 CCC: $33.50
Published on Web 04/04/2006

conformation which is very flexible. In that conformation, the three OMe or OEt groups are flattened and point toward the center of the cavity, while OR_2 groups stand up. This disposition reduces the size of the cavity and the flexibility of the structure. On the other hand, an increase of the size of the lower rim substituents favors the 1,2,3-alternate conformation that corresponds to a lower (C_s) symmetry. However, an interconversion with the cone conformation can still occur via the *p-tert*-butyl through the annulus pathway.[23,25] Similar conclusions have been obtained using chromatographic techniques (HPLC) with chiral packed columns.[26]

Despite this impressive amount of experimental studies, many issues still remain unclear. For instance, the influence of the solvent, the role of the counterion, and the shape of the conformational space of the unbound forms are not well understood. At the same time, a straightforward interpretation of the experimental results is not always possible, since the overall physicochemical properties are often the result of a delicate balance among different structural, electronic, and environmental effects.[27] In such circumstances, theoretical predictions offer an important support. From a theoretical point of view, small calixarenes, as those belonging to the calix[4]-arene family, have been widely studied using either empirical or semiempirical techniques.[28−32] In particular, molecular dynamic simulations have been employed to study the interaction of alkaline cations with calix[4]arenes[29,30] and solvation effects on the conformational isomerism of these molecules.[31] More recently, first-principles approaches have been used to get a deeper insight into the structural and spectroscopic properties of these molecules. For example, several works report the theoretical analysis of the equilibrium conformations of calix[4]arenes[33−37] or the calculations of NMR chemical shifts.[36] Infrared spectra have also been calculated using simplified molecular models.[37,38] Finally, solvent effects on the conformational behavior of calix[4]arenes were introduced at the semiempirical level, using a continuum polarizable model.[39]

The size of the systems under investigation makes troublesome detailed quantum mechanical studies of the large members of the calix[*n*]arene family. Therefore, it is not surprising that theoretical calculations are very rare for the largest members of the calix[*n*]arene family, like the calix[6]arenes. To the best of our knowledge, only empirical calculations based on the molecular mechanics approach are reported in the literature.[40,41] In particular, Yuan and co-workers compared the stabilities of 1,3,5-OMe-2,4,6-OR-*p-tert*-butylcalix[6]arenes in C_{3v} and C_s conformations.[40] They found that the most stable conformer has a C_{3v} structure corresponding to a flattened cone conformation, while other conformers such as the C_s 1,2,3-alternate isomer are much higher in energy. More recently, Oshima et al. studied the structure of the complex between amino acid esters and a calix[6]arene with a semiempirical method.[42] They calculated the chemical shift of protons, assigning the $Ar-CH_2-Ar$ methylene bridge of the calix[6]arene using the Hartree−Fock method.

A detailed theoretical and experimental study on the conformational analysis of the 1,3,5-OMe-2,4,6-$OCH_2CONHOH$-*p-tert*-butylcalix[6]arene is presented in this paper. The aim of this study is to obtain direct structure/properties relationships, in order to have a clear picture of the conformational behavior of this calix[6]arene. To this end, the most stable conformers have been identified using both semiempirical and density functional theory (DFT) approaches. Then, ^1H and ^{13}C NMR experiments have been carried out to further characterize this molecule, following the classical protocol to determine the conformations of calix[*n*]arenes. Finally, the ^1H and ^{13}C NMR spectra on model systems, namely, two successive phenol rings ($Ar_1-CH_2-Ar_2$), have also been computed at the DFT level and compared with the experimental spectra of the complete molecule. A study about the effect of the angle between the two rings on the chemical shift of the methylene carbon has also been performed. These calculations allow comparison of the stability of the different conformations, a comparison which is not always straightforward by NMR experimental studies,[26,43] and improvement of the knowledge of complexation properties as a function of the geometry and of the functionalized groups. In this way, our calculations can be used as a comparative, if not predictive, tool with respect to chemical experiments.

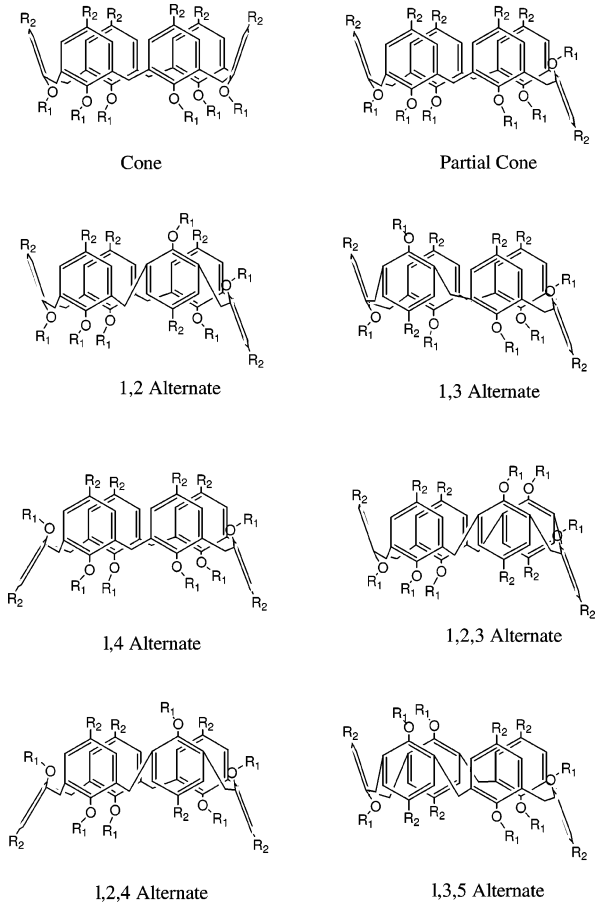

Figure 2. Sketches and labeling of the considered conformational isomers of calix[6]arenas. Hydrogen atoms are omitted for clarity.

2. Computational Details

All calculations were carried out with the Gaussian code.[44] The eight selected systems (Figure 2) have been fully optimized at the semiempirical level using the Austin model approach (AM1). Hence, single-point DFT calculations were carried out using the so-called PBE0 "parameter free" hybrid model.[45] This model is derived by casting the Perdew−Burke−Enrzerhof (PBE) exchange-correlation functional[46] in a hybrid HF/DFT scheme, where the HF exchange ratio ($^1/_4$) is fixed a priori.[47] We used a standard polarized 6-31G(d) basis set for all atoms.[48] Additional geometry optimizations were carried for selected conformations (five), using the PBE0 functional and the same basis sets.

NMR calculations were realized using the GIAO approach, as implemented in the Gaussian program,[49] at the DFT level. Two different basis sets have been considered: the 6-31G(d,p)

basis set already used for geometry optimizations and the larger 6-31+G(2d,2p) basis set. This latter basis set provides chemical shifts at convergence.[49] All the NMR results were given as chemical shifts (δ) of the atom (X = C or H) with respect to the values of the corresponding atoms in DMSO.

Finally, solvent effects were evaluated using the polarizable continuum model (PCM).[50] Solvation energies have been computed by a cavity model, namely, the united atoms topological model (UATM),[51] coupled to the conductor-like polarizable continuum model (CPCM).[52]

3. Experiment Details

1,3,5-OMe-2,4,6$OCH_2CONHOH$-*p-tert*-butylcalix[6]arene has been synthesized by Chelator S.A. (France) in collaboration with Claude-Bernard Lyon 1 University (France). ^1H and ^{13}C NMR spectra were recorded in DMSO-d_6 and in CD_2Cl_2 on a Bruker Avance 400 MHz spectrometer at 298 K.

4. Results and Discussion

As mentioned in the Introduction, NMR spectra are used to characterize the conformational behavior of calix[*n*]arenes. In ^1H NMR spectra, the characteristic conformational signals are, for example, those of Ar−CH_2−Ar, *p-tert*-butyl, OCH_3, or aromatic protons as well as their multiplicities.[20−23] These signals are directly related to the symmetry (C_{3v}, C_s, and nonsymmetric) of the molecule.[23] For instance, the multiplicity in the ^1H NMR spectra of the OMe group of 1,3,5-OMe-2,4,6-OR-*p-tert*-butylcalix[6]arenes is one singlet when the conformation has a C_{3v} symmetry (flexible conformer) and two singlets for a C_s conformation. The number of peaks of the methylene protons of Ar−CH_2−Ar is two doublets for a C_{3v} conformation, six doublets for C_s, and one singlet for a flexible conformation .[23] In ^{13}C NMR, the conformation of calixarenes can be easily determinated with the shift of the Ar−CH_2−Ar methylene-bridged carbon. When the phenol rings beside methylene are in a syn orientation, i.e., in cone conformation, the methylene signal appears around 31 ppm, whereas it appears around 37 ppm when both phenyl rings are anti oriented.[24] Steric effects are believed to be the main cause of such large differences, because literature X-ray data of calix[4]arenes show that the angle C(sp2)−C(sp3)−C(sp2) is always smaller for syn orientation (107−111°) than for anti orientation (111−118°).[25] However, one type of calixarenes for which this rule is not working is reported. For partially substituted calix[4]arenes, the ^{13}C NMR shift of the methylene carbons are midway between the standard 31 and 37 ppm values for "pure" syn or anti arrangements.[53] This difference has been attributed either to a distorted fixed conformation or a fast equilibrium between syn and anti arrangements. All the configurations accessible for the 1,3,5-OMe-2,4,6-$OCH_2CONHOH$-*p-tert*-butylcalix[6]arene and considered in the present paper are sketched in Figure 2. Following previous works,[20,25,26,43] we adopted the following nomenclature: cone, partial-cone (hereafter referred to as paco), 1,2-alternate (12alt), 1,3-alternate (13alt), 1,4-alternate (14alt), 1,2,3-alterante (123alt), 1,2,4-alternate (124alt), and 1,3,5-alternate (135alt).

4.1. Conformational Behavior: Theoretical Energetic Analysis. Following previous works,[39] a first rough exploration of the conformational space of the eight conformers of the 1,3,5-OMe-2,4,6-$OCH_2CONHOH$-*p-tert*-butylcalix[6]arene was carried out using the semiempirical AM1 approach. The eight conformations sketched in Figure 2 were fully optimized, and the stationary points found were characterized as true energy minima by frequency calculations. The structures obtained for five of the investigated conformers (cone, 123alt, 12alt, 13alt, and paco) are reported in Figures 1 and 3. The energy differences are collected in Table 1, taking as reference the energy of the cone structure. Indeed, as already obtained for smaller calixarenes,[43] the cone structure (Figure 1) is the most stable, but the energy differences of the four other conformations (123alt, 12alt, 13alt, and 14alt) are within 10 kcal/mol. These structures differ in the size of the cage and the availability of the hydroxamic group, both parameters being of primary relevance for host−guest interactions. The relative stabilities are mainly ruled by two concurrent effects: the steric hindrance of the *tert*-butyl groups bonded to the phenyl rings and the H-bond network formed by the $CH_2CONHOH$ groups. Therefore, a correct description of the conformational behavior of such structures requires an adequate description of both concomitant interactions. While the first effect (steric hindrance) can be easily modeled and can be assumed to be correctly reproduced at the AM1 level,[54] the second one, H-bonding, is more troublesome.[55,56]

TABLE 1: Relative Energies (ΔE, kcal/mol) of the Eight Most Stable Conformers of 1,3,5-OMe-2,4,6-$OCH_2CONHOH$-*p-tert*-butylcalix[6]arene, with Respect to the Energy of the Cone Conformer

geometry//energy	cone	123alt	12alt	13alt	14alt	paco	124alt	135alt
AM1//AM1	0.0	2.8	5.4	9.2	9.5	12.7	16.1	17.2
DFT//AM1	0.0	7.6	1.9	7.8	20.2	5.8	15.8	10.3
DFT//DFT	0.0	19.2	0.1	9.0		6.5		
DFT//DFT in CCl_4	0.0		2.3			8.1		
DFT//DFT in $CHCl_3$	0.0		3.6			8.4		
DFT//DFT in DMSO	0.0		4.3			8.4		

Since in many cases AM1 geometries are still reasonable, single-point calculations were performed at DFT level on the optimized AM1 structures in order to verify the already found order of stability between the different conformers. The results are listed in Table 1. These data show that both theoretical levels indicate the cone conformation as the most stable one. In contrast, a different order is suggested by DFT. In fact, the paco and 135alt conformations are significantly stabilized in going from AM1 to DFT ($\Delta\Delta E_{rel} = -6.9$ kcal/mol), and to a minor extent, the relative energies of the 12alt and 13alt conformations decrease ($\Delta\Delta E_{rel} = -3.5$ and -1.4, respectively). At the same time, the 14alt and 123alt conformations increase their relative energies with respect to the cone conformation ($\Delta\Delta E_{rel} = +4.8$ and 10.7 kcal/mol, respectively). This effect could be ascribed to a better description of the H-bond interactions ruling the geometry of the cage.

Starting from these AM1 structures, we decided to fully characterize at DFT level the five most stable conformers, among those already studied. The results are reported in the third line of Table 1. The most striking feature is the large destabilization of the 123alt conformer, which is predicted to be about 19 kcal/mol higher in energy than the cone conformer. In contrast, minor variations, about 2 kcal/mol, are observed for the other conformers. It must be noted, anyway, that DFT calculations predict the 12alt to be almost isoenergetic ($\Delta E_{rel} = 0.1$ kcal/mol) with the cone conformer. In any case, the AM1 and the DFT geometries are very similar, as can be seen in Figure 4 where the superimposition of the two 123alt conformations (AM1 and DFT) is reported.

The relative stabilities of the different conformers can be easily related to the number of the intramolecular H-bonds between different groups. In particular, three H-bonds are present in the cone conformation (two between OMe and hydroxamic groups and one between two different hydroxamic groups) as in the 12alt isomer (two $CH_2CONHOH$−$CH_2CONHOH$ and

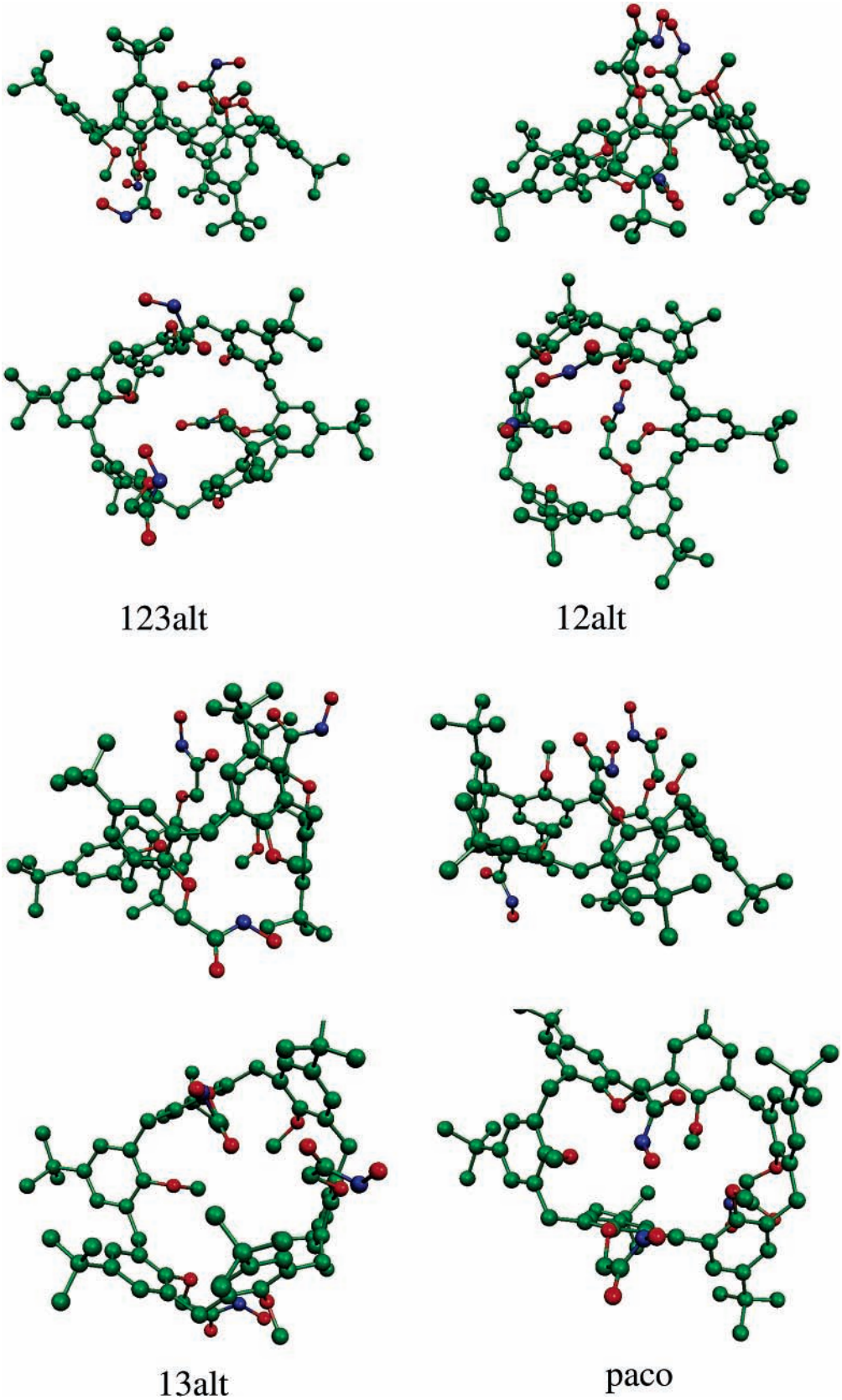

Figure 3. Structures of the four most stable conformers (above the cone conformer) of the 1,3,5-OMe-2,4,6-$OCH_2CONHOH$-*p-tert*-butylcalix-[6]arene.

one OMe-$CH_2CONHOH$), thus explaining why the two structures are isoenergetic at the DFT level. Then, the paco structure, the third in the stability order, has two H-bonds (between OMe and $CH_2CONHOH$ and between two different hydroxamic groups), while the 13alt shows just one H-bond (between OMe and $CH_2CONHOH$).

Therefore, the energy discrepancies between the AM1 and DFT results can be attributed to the diverse ways of treating

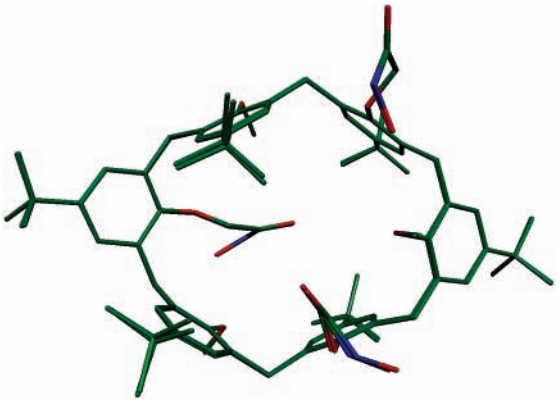

Figure 4. Superimposition of the AM1 and DFT structures of the 123alt isomer.

intramolecular forces and, in particular, H-bonds, ruling the conformational behavior of calix[6]arenes. This is not surprising, since it is well-known that AM1 significantly overestimates H-bonding,[56] while the PBE0 approach provides a more correct description.[57]

To study the solvent effect on the conformational stability, single-point energy calculations in DMSO, $CHCl_3$, and CCl_4 were performed at DFT level on the three most stable DFT structures. The results are reported in the last three lines of Table 1. Significant variations can be observed in the relative energy order upon the addition of the solvent reaction field. In particular, the energy gap between the cone and the 12alt conformations significantly increases from 0.1 to 3.6 kcal/mol in $CHCl_3$. A smaller variation (+2.0 kcal/mol) is computed for the paco conformer. It is interesting to note that when a solvent with a higher dielectric constant is considered (here, DMSO) the former difference further increases (from 3.6 to 4.3 kcal/mol), while the paco conformer is not affected. We also want to note that in such systems solvents effects cannot be easily analyzed in terms of the dipole moments of the different conformers. In fact, the paco structure has a gas-phase dipole moment comparable to that of cone (11.6 and 14.8 D, respectively) but seems to be less stabilized by the continuum than the 12alt, bearing a lower dipole moment (1.8 D).

In summary, our calculations confirm that the cone conformer is the most stable conformer of 1,3,5-OMe-2,4,6-$OCH_2CONHOH$-*p-tert*-butylcalix[6]arene, while the other structures are higher in energy. Furthermore, the calculations show that in the presence of a polar solvent the cone conformer is the only species in solution. As the dielectric constant decreases toward 1, the cone and the 12alt conformers tend to become almost isoenergetic, and thus, both are present in solution. Even if some crude approximations are behind the continuum model, our results suggest a non-negligible role of the solvent in the stabilization of the different conformers. At the same time, these results show the significant qualitative and quantitative differences between ab initio (DFT) and semiempirical (AM1) calculations, in particular, concerning the relative energies of the conformers.

4.2. Conformational Behavior: The Experimental NMR Signature. From the above calculation and in order to better investigate the role of the solvent on the conformation equilibrium, ^1H and ^{13}C NMR experimental spectra have been recorded in DMSO-d_6 at room temperature (Figure 5).

The ^1H chemical shifts (ppm) are as follows: 10.84 and 9.07 (two s, 6H, −NHOH), 7.31 (s, 6H, ArH/*meta*-OCH_3), 6.57 (s, 6H, ArH/*meta*-$OCH_2CONHOH$), 4.41 (d, 6H axial) and 3.45 (d, 6H equatorial, $ArCH_2Ar$), 4.30 (s, 6H, $-OCH_2CO$), 2.07 (s, 9H, $-OCH_3$), 1.36 (s, 27H, $C(CH_3)_3$/*para*-OCH_3), and 0.73 (two s, 54H, $C(CH_3)_3$/*para*-$OCH_2CONHOH$).

The number of signals is characteristic of the C_{3v} symmetry of 1,3,5-OMe-2,4,6-$OCH_2CONHOH$-*p-tert*-butylcalix[6]arene. The signature of the NMR ^1H spectra clearly shows the presence of one major conformer in DMSO that can be assigned to the cone structure. The ^{13}C chemical shift of the fragment $Ar_1-CH_2-Ar_2$ in DMSO-d_6 at 29.21 ppm confirms the presence of the cone conformation in this solvent.

Then,^1H and ^{13}C NMR experimental spectra have been recorded in CD_2Cl_2 at 298 K (Figure 6). The attribution of the ^1H signals is difficult because of the number of the peaks and

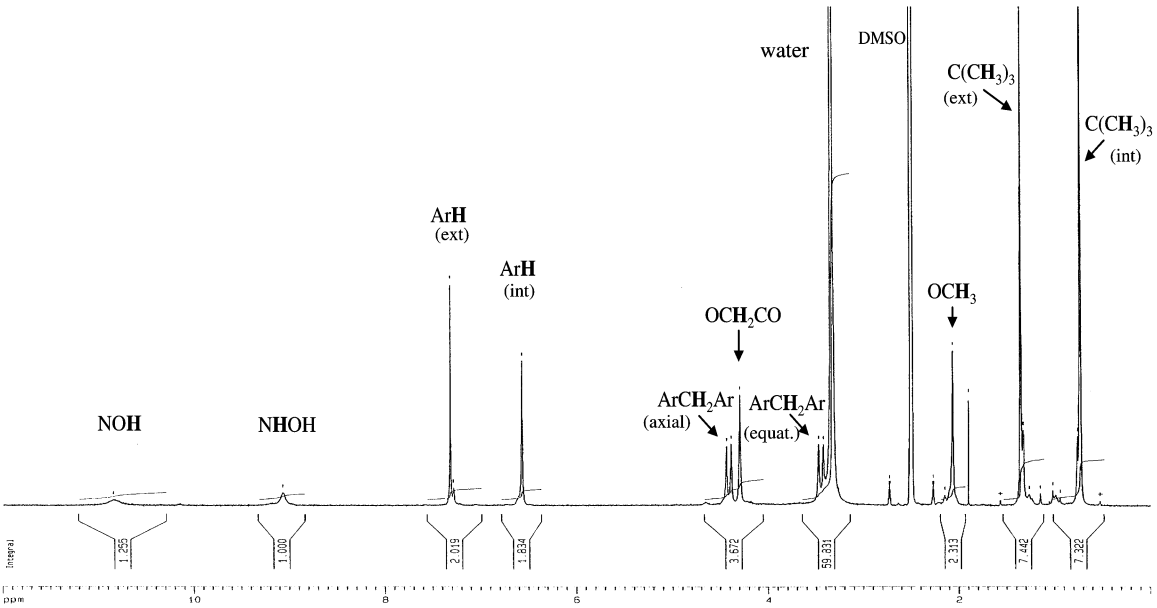

Figure 5. Experimental ^1H NMR spectrum in DMSO-d_6 of the 1,3,5-OMe-2,4,6-$OCH_2CONHOH$-*p-tert*-butylcalix[6]arene.

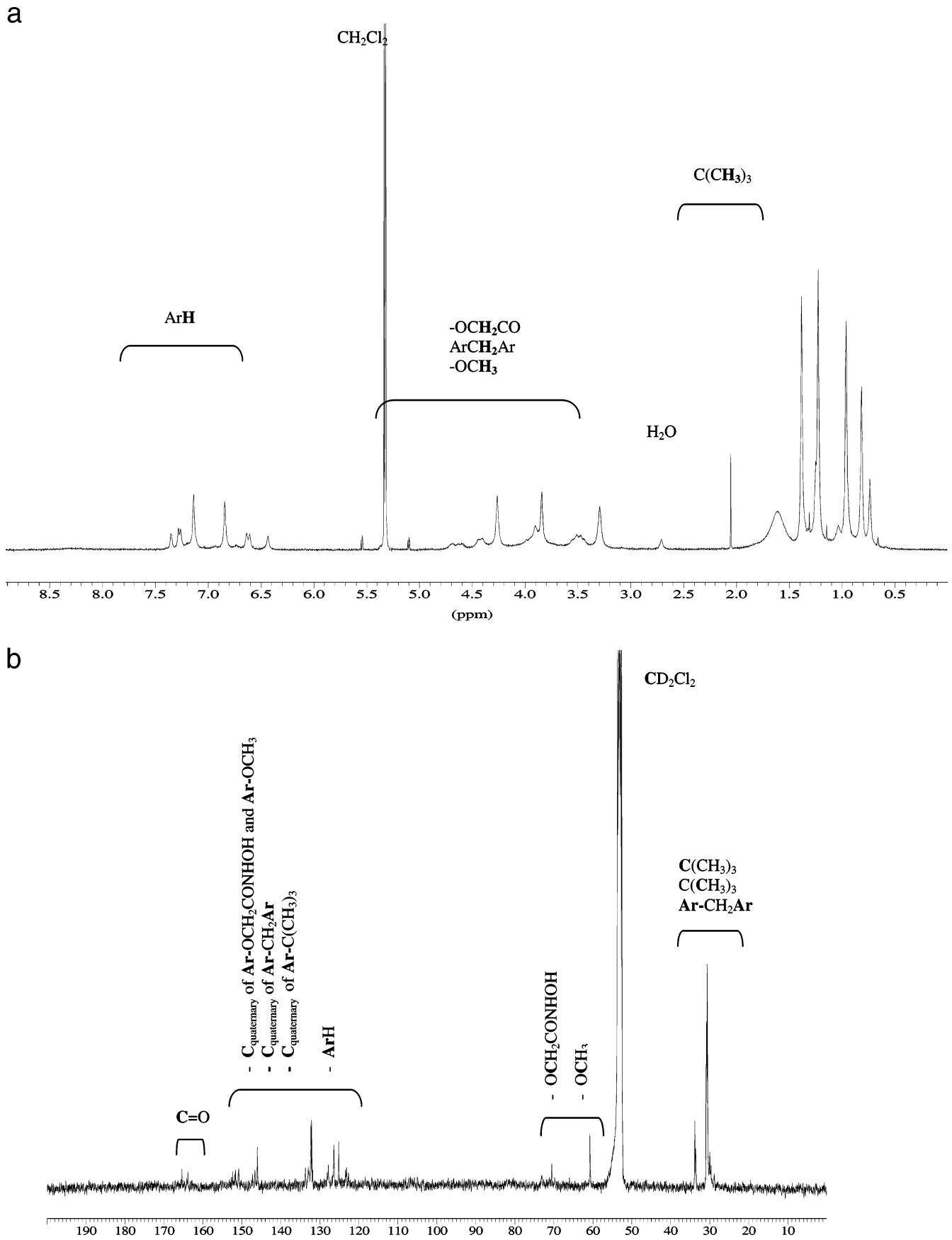

Figure 6. Experimental ^1H (a) and ^{13}C (b) NMR spectra in CD_2Cl_2 of the 1,3,5-OMe-2,4,6-$OCH_2CONHOH$-*p*-*tert*-butylcalix[6]arene.

their weak intensities. Even if, in principle, more information could be obtained by 2D-NMR analysis, the weak signals, coupled with the low solubility of the calix[6]arene in CD_2Cl_2, prevent this kind of experiment (at least in a reasonable time). However, three areas can be defined: between 7.35 ppm and 6.60 ppm (ArH), between 4.5 ppm and 2.70 ppm (OCH_2, $ArCH_2Ar$, and OCH_3), and between 1.38 ppm and 0.70 ppm ($C(CH_3)_3$).

Thus, in the ^{1}H NMR spectrum in CD_2Cl_2, several conformations are observed, but none of them can be clearly attributed. Therefore, in an attempt to determine the major conformation in CD_2Cl_2, a ^{13}C NMR spectrum has been realized. After 2 days of recording, the attribution of the ^{13}C signals is still difficult principally because of the weak intensity of the signals (Figure 6). In addition, the concentration of the product could not be increased because of its weak solubility in CD_2Cl_2. Four areas can be defined: at 164.6 ppm (C═O), between 153 and 122 ppm (quaternary carbons and aromatic CH), between 70.5 and 60 ppm (OCH_2 and OCH_3), and between 33.8 and 28 ppm ($C(CH_3)_3$, $ArCH_2Ar$, and $C(CH_3)_3$). Unfortunately, from this spectrum, we can only conclude that several conformations are present in this solvent, but clear assignments were not possible.

In summary, one major conformation (cone) can be observed in a polar solvent as DMSO but not in a less polar solvent, as CD_2Cl_2, where a mix of different conformations is found. This phenomenon may be explained by a significant stabilization of the cone structure due to the electrostatic interactions with the polar solvent. This last result is in good qualitative agreement with the theoretical predictions discussed in the previous paragraph. In addition, these experimental results clearly show the difficulty in attributing all the calix[6]arene conformations from NMR experimental spectra.

4.3. Conformational Behavior: The Theoretical NMR Signature. Experimental suggestions indicate that the ^{13}C chemical shifts are around 30 ppm, when two adjacent phenyl rings are in the syn position and around 40 ppm in the anti position. Unfortunately, the size of the calix[6]arenes makes first-principles NMR calculations extremely time-consuming, even at the DFT level with a small basis set. Therefore, following the experimental indications, it has been argued that, instead of calculating the NMR spectra of the whole calix[*n*]-arenes, it is sufficient to analyze the chemical shifts in smaller fragments.[36,42] In this line, we have studied only a part of the whole calix[6]arene, namely, the fragment $Ar_1-CH_2-Ar_2$ with Ar_1 = OMe-*p*-*tert*-butylphenyl and Ar_2 = $OCH_2CONHOH$-*p*-*tert*-butylphenyl. So the overall conformational behavior of the calix[6]arene can be reduced to the analysis of the transition from the syn to the anti isomer of $Ar_1-CH_2-Ar_2$, reported in Figure 7. As a first step in this direction, we have verified this approach by computing the ^{1}H and ^{13}C spectra on the $Ar_1-CH_2-Ar_2$ motif extracted from the cone conformer. To have a complete picture of the problem, we have computed the chemical shifts using two different basis sets and both AM1 and DFT optimized geometries. The results are collected in Tables 2 and 3. Before analyzation of these data, we want to point out that the conformation behavior of calix[6]arene has been also studied, at the experimental level, using the ^{1}H chemical shifts of the hydrogens belonging to the *tert*-butyl (*t*-Bu), aromatic (ArH), and OCH_3 (OMe) substituents.[21,58] Nevertheless, these shifts are strongly affected by the anisotropic cone generated by the aromatic cycles. Since this effect is obviously missing in our model systems, these parameters will be relatively poorly reproduced.

Let us start from the ^{1}H chemical shifts (δ), reported in Table 2, for which a comparison with experiments is possible. From the values collected in this table, it appears that there is an overall good agreement with the experimental data, whatever the geometry (AM1 or DFT) or the basis (6-31G(d) or 6-31+G-(2d,2p)) used. Nevertheless, the best results have been obtained with the DFT geometry and the small basis set (fourth column of Table 2). In this case, the calculated chemical shifts of *tert*-butyl are 1 ppm higher than the experimental values. Similar

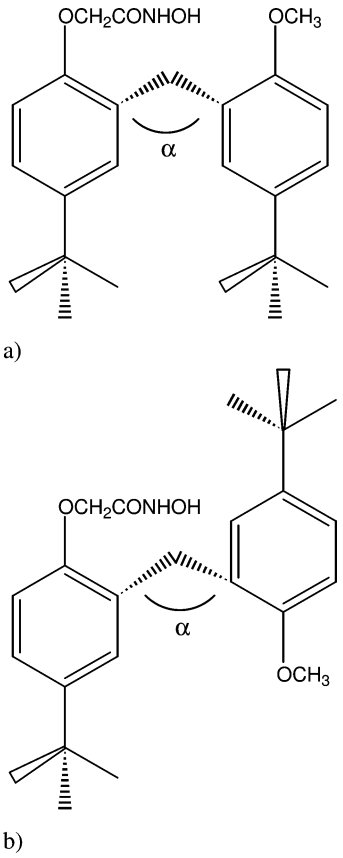

Figure 7. System models used in NMR calculations: (a) syn oriented; (b) anti oriented.

TABLE 2: Computed ^{1}H Chemical Shifts (δ, ppm) of the Fragment $Ar_1-CH_2-Ar_2$ with Ar_1 = OMe-*p*-*tert*-butylphenyl and Ar_2 = $OCH_2CONHOH$-*p*-*tert*-butylphenyl and Experimental ^{1}H Chemical Shifts (δ, ppm) of the Most Stable Conformation (cone) of 1,3,5-OMe-2,4,6-$OCH_2CONHOH$-*p*-*tert*-butylcalix[6]arene in DMSO-d_6[a]

atom	DFT//AM1[b]	DFT//AM1[c]	DFT//DFT[c]	exp
t-Bu (OMe)	2.5	2.2	1.6	0.7
t-Bu (hydrox)	2.6	2.3	1.7	1.4
N*H*O*H*	4.4	4.9	8.5	10.9
NH	9.3	9.3	11.3	9.1
$ArCH_2Ar$	5.8	5.8	5.0	4.4
	4.5	4.5	3.9	3.5
OMe	5.0	4.9	4.3	2.1
OCH_2	5.5	5.5	4.8	4.3
ArH(OMe)	7.7	8.0	8.0	6.6
ArH(hydrox)	7.8	8.0	8.0	7.3

[a] All the values are reported as average over (pseudo)equivalent atoms. [b] 6-31G(d,p) basis set. [c] 6-31+G(2d,2p).

discrepancies have been found for the protons of the methylene groups ($ArCH_2Ar$ and OCH_2) and the aryl hydrogens (between 0.7 and 1.4 ppm) As mentioned before, this discrepancy could be mainly ascribed to the limited size of our model, which does not correctly model overall molecular effects on the ^{1}H shifts. At the same time, the largest computed deviations are for the NOH protons, about 2 ppm away from the experimental data. Since these protons are quite acidic, the difference could be attributed to hydrogen bonds or solvent effects.

Small variations are observed in going from the DFT to the AM1 structures, with the exception of the two hydrogens of the hydroxamicgroup (N*H*O*H*, in Table 2). Finally, the comparison of the two data sets obtained with the AM1 geometry and the different basis sets show the negligible effect due to

TABLE 3: Computed ^{13}C Chemical Shifts (δ, ppm) of the Fragment $Ar_1-CH_2-Ar_2$ with Ar_1 = OMe-*p*-*tert*-butylphenyl and Ar_2 = $OCH_2CONHOH$-*p*-*tert*-butylphenyl and Experimental ^{13}C Chemical Shifts (δ, ppm) of the Most Stable Conformation (cone) of 1,3,5-OMe-2,4,6-$OCH_2CONHOH$-*p*-*tert*-butylcalix[6]arene in DMSO-d_6[a]

atom	DFT//AM1[b]	DFT//AM1[c]	DFT//DFT[c]	exp
ArH(hydrox)	123.2	119.8	122.0	128.4
ArH(OMe)	122.5	119.3	122.1	123.3
$ArCH_2Ar$	33.5	31.0	28.1	29.2
OCH_2	79.1	77.4	72.8	70.7
OMe	66.2	65.0	62.7	59.8
t-Bu (hydrox)	37.6	35.4	30.0	31.7
t-Bu (OMe)	37.6	35.2	29.9	31.1

[a] All the values are reported as averages over (pseudo)equivalent atoms. [b] 6-31G(d,p) basis set. [c] 6-31+G(2d,2p).

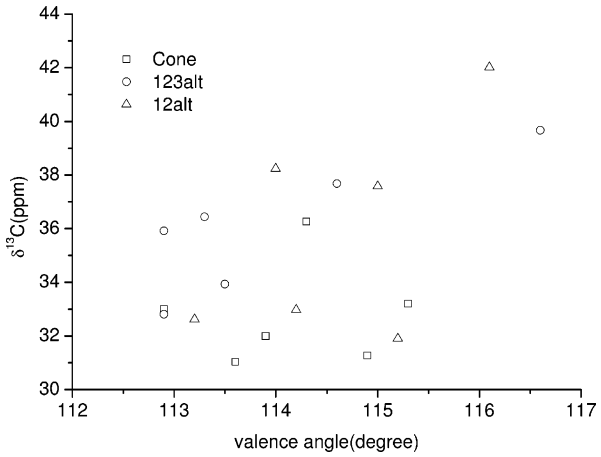

Figure 8. Plot of the ^{13}C chemical shift of the carbon atom embedded in the $Ar-CH_2-Ar$ motif extracted from the three most stable conformers of the calix[6]arene as function of the valence angle.

the enlargement of the basis. Similar trends have been found for the $\delta(^{13}C)$ values, as it can be seen from the data reported in Table 3. Here, as already noticed in the literature,[59] a better agreement is found between theoretical and experimental data. The largest difference (about 6 ppm) is found for the aryl carbons. A more important result is that the chemical shift of the methylene carbon ($ArCH_2Ar$) is reproduced with an accuracy of 1 ppm, an error smaller than the variation used to assign the conformer. This value, as expected for syn oriented groups, is close to 30 ppm.

Then, to better investigate the effects of conformational changes on the NMR spectra, we have extracted different pairs of $Ar_1-CH_2-Ar_2$ fragments from the cone, 12alt, and 123alt conformations. On such structures, we have calculated the ^{13}C NMR spectra at the DFT level, with the 6-31G(d,p) basis set. The results are reported in Figures 8 and 9, as a function of the valence angle $C(Ar_1)-CH_2-C(Ar_2)$ and of the torsion angle (τ) around the Ar_1-CH_2 bond, respectively. There is no direct relationship between the valence angles and the computed chemical shifts of ^{13}C, since for the same angle, the difference in the shifts can be relatively large (up to 8 ppm). The behavior of the δ's with respect to the torsion angle is more regular (Figure 9). In fact, two regions of chemical shifts can be localized in this figure: one region between 30 and 34 ppm and another between 36 and 40 ppm. The first region corresponds, of course, to the aromatic groups in the syn position and the second one to the anti rearrangement. Nevertheless, there is no direct connection between the torsion angle and δ of ^{13}C. This apparent discrepancy can be easily explained by looking

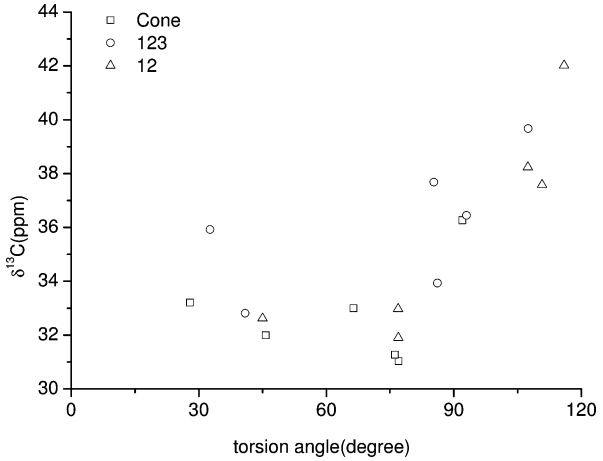

Figure 9. Plot of the ^{13}C chemical shift of the carbon atom embedded in the $Ar-CH_2-Ar$ motif extracted from the three most stable conformers of the calix[6]arene as a function of the absolute value of the torsion angle.

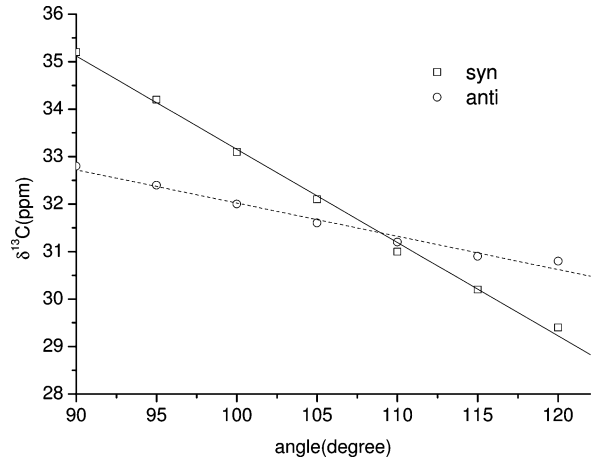

Figure 10. Plot of the ^{13}C chemical shift of the carbon atom embedded in the $Ar-CH_2-Ar$ motif for the anti and syn models as a function of the valence angle.

at typical rearrangements of the $Ar_1-CH_2-Ar_2$, as those reported in Figure 3. For these structures, the arrangement is clearly either syn or anti, but due to the constraints of the calixarene conformation, the torsion angles are close for the two species.

To better clarify this point, we have studied the variation of the chemical shifts of the methylene carbon as a function of the valence and the torsion angles. The calculations have been done using optimized structures at the DFT level, and the results are collected in Figures 10 and 11. In the former case the results show a perfect linear correlation between the valence angle and the computed δ's both for the anti (R = 0.991) and for the syn (R = 0.999) conformations. It must be pointed out that a relatively large variation is found for the shifts ($\Delta\delta$ values of about 6 ppm for syn and 2 ppm for anti) in the range of the considered valence angles (90−120°). The δ variation is much smaller with respect to that computed with the optimized structures (14 ppm) when the range of the optimized valence angles is considered (112−117°, in Figure 8).

In a similar manner, a small variation ($\Delta\delta$ = 5 ppm) is found for a large interval of the torsion angles (−60−100) (Figure 11), whereas a larger effect is found in the case of the optimized structures (up to 12 ppm, Figure 9). Both results show how the chemical shift of the methylene carbon is ruled by concomitant geometrical effects, beyond the two considered angles.

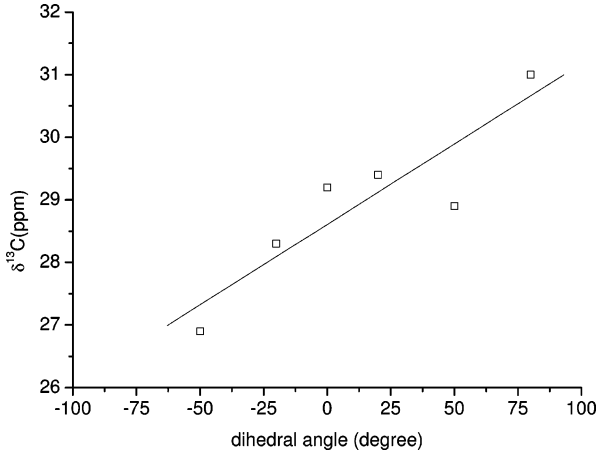

Figure 11. Plot of the ^{13}C chemical shift of the carbon atom embedded in the $Ar-CH_2-Ar$ motif for the anti and syn models as a function of the dihedral angle.

In summary, the experimental hypothesis of a direct relationship between the conformational behavior of the calix[*n*]arenes and the chemical shifts of the bridging methylene carbon atoms should be correct. Nevertheless, geometrical constraints could force different torsion angles, so that the observed shifts are difficultly assigned to one specific conformer among the possible ones. This effect is not only evaluated at theoretical level, but also, it is present when NMR spectra are recorded in different solvents.

5. Conclusion

In this paper, we have presented a detailed theoretical and experimental study on the conformational analysis of the 1,3,5-OMe-2,4,6-$OCH_2CONHOH$-*p*-*tert*-butylcalix[6]arene. Semiempirical (AM1) and DFT calculations have been carried out in order to identify the most stable conformers. Even if the two levels of theory predict the cone structure to be the most stable one, significant differences have been reported for the other species. The results point out the need of the DFT to evaluate both structure and properties. Our calculations also show the relevant role played by the solvent on the stabilization of the different species in solution. These last results have been confirmed by NMR experiments. In particular, ^1H NMR experimental spectra in DMSO-d_6 and in CD_2Cl_2 show the solvent effect on the calixarene conformations. In the DMSO, the calixarene appears frozen into the cone conformation, whereas in the CD_2Cl_2, the flexibility of the calixarene is free and several conformations appear in the spectra at ambient temperature.

The ^1H and ^{13}C NMR spectra on model systems, namely, two successive phenol rings ($Ar_1-CH_2-Ar_2$), have been computed at the DFT level and compared with the experimental spectra of the complete molecule. There is an overall good agreement with the experimental data, regardless of the model system geometry (AM1 or DFT) or the basis set (6-31G(d) or 6-31+G(2d,2p)) used.

Finally, we have tried to elucidate the well-known rule between the ^{13}C chemical shift of the bridging methylene carbon and the calixarene conformation. The results show how the chemical shift of the methylene carbon is ruled by concomitant geometrical effects, beyond the valence and the torsion angles.

Acknowledgment. Authors thank CINES (project no. ECA2515) and IDRIS (project no. 051830) for generous grants of computer time.

References and Notes

(1) Gutsche, C. D. *Calixarenes Revisited*; The Royal Society of Chemistry: Cambridge, 1998.
(2) Ludwig, R.; Kunogi, K.; Dung, N.; Tachimori, S. *Chem. Commun.* **1997**, 1985.
(3) Lambert, T. N.; Jarvinen, G. D.; Gopalan, A. S. *Tetrahedron Lett.* **1999**, *40*, 1613.
(4) Arnaud-Neu, F.; Schwing-Weill, M. J. *Synth. Met.* **1997**, *90*, 157.
(5) Havrlock, T. J.; Mirzadeh S.; Moyer, B. A. *J. Am. Chem. Soc.* **2003**, *125*, 1126.
(6) Lambert, B.; Jacques, V.; Shivanyuk, A.; Matthews, S. E.; Tunayar, A.; Baaden, M.; Wipff, G.; Böhmer, V.; Desreux, J. F. *Inorg. Chem.* **2000**, *39*, 2033.
(7) Araki, K.; Hashimoto, N.; Otsuka, H.; Nagasaki, T.; Shinkai, S. *Chem. Lett.* **1993**, 829.
(8) Nagasaki, T.; Shinkai, S. *J. Chem. Soc., Perkin Trans. 2* **1991**, *1063.*
(9) Shinkai, S.; Koreishi, H.; Ueda, K.; Arimura, T.; Manabe, O. *J. Am. Chem. Soc.* **1987**, *109*, 6371.
(10) Shinkai, S.; Shiramama, Y.; Satoh, H.; Manabe, O. *J. Chem. Soc., Perkin Trans. 2* **1989**, 1167.
(11) Nagasaki, T.; Shinkai, S.; Matsuda, T. *J. Chem. Soc., Perkin Trans. 1* **1990**, 2617.
(12) Nagasaki, T.; Shinkai, S. *J. Chem. Soc., Perkin Trans. 2* **1991**, 1063.
(13) Araki, K.; Hashimoto, N.; Otsuka, H.; Nagasaki, T.; Shinkai, S. *Chem. Lett.* **1993**, 829.
(14) Baglan, N.; Dinse, C.; Cossonnet, C.; Abidi, R.; Asfari, Z.; Leroy, M.; Vicens, J. *J. Radioanal. Nucl. Chem.* **1997**, *226* (1−2), 261.
(15) Dinse, C.; Baglan, N.; Cossonnet, C.; Le Du, J. F.; Asfari, Z.; Vicens, J. *J. Alloys Compd.* **1998**, *271*−*273*, 778.
(16) Dinse, C.; Baglan, N.; Cossonnet, C.; Bouvier, C. *Appl. Radiat. Isot.* **2000**, *53*, 381.
(17) Souane, R.; Hubscher, V.; Asfari, Z., Arnaud, F.; Vicens, J. *Tetrahedron Lett.* **2003**, *44*, 9061.
(18) Agrawal, Y. K.; Sanyal, M. *J. Radioanal. Nucl. Chem.* **1995**, *198* (2), 349.
(19) Gutsche, C. D. *Calixarenes*; The Royal Society of Chemistry: Cambridge, 1989.
(20) Gutsche, C. D.; Bauer, L. J. *J. Am. Chem. Soc.* **1985**, *107*, 6059.
(21) Sénequé, O.; Rondelez, Y.; Le Clainche, L.; Inisan, L.; Rager, M.-N.;; Giorgi, M.; Reinaud, O. *Eur. J. Inorg. Chem.* **2001**, 2597.
(22) Casnati, A.; Minari, P.; Pochini, A.; Ungaro, R. *J. Chem. Soc., Chem. Commun.* **1991**, 1413.
(23) van Duynhoven, J. P. M.; Janssen, R. G.; Verboom, W.; Franken, S. M.; Casnati, A.; Pochini, A.; Ungaro, R.; de Mendoza, J.; Nieto, P. M.; Prados, P.; Reinhoudt, D. N. *J. Am. Chem. Soc.* **1994**, *116*, 13, 5814.
(24) Jaime, C.; de Mendoza, J.; Prados, P.; Nieto, P. M.; Sanchez, C. *J. Org. Chem.* **1991**, *56*, 3372.
(25) Ikeda, A.; Shinkai, S. *Chem. Rev.* **1997**, *97*, 1713.
(26) Otsuka, H.; Araki, K.; Sakaki, T.; Nakashima, K.; Shinkai, S. *Tetrahedron Lett.* **1993**, *34*, 45, 7275.
(27) Improta, R.; Barone, V. *Chem. Rev.* **2004**, *104* 1231.
(28) Shinkai, S.; Iwamoto, K.; Araki, K.; Matsuda, T. *Chem. Lett.* **1990**, 1263.
(29) Baaden, M.; Wipff, G.; Yaftian, M. R.; Burgard, M.; Matt, D. *J. Chem. Soc., Perkin Trans. 2* **2000**, 1315.
(30) Guilbaud, P.; Wipff, G. *J. Am. Chem. Soc.*, **1993**, *115*, 8298.
(31) van Hoorn, W. P.; Briels, W. J.; van Duynhoven, J. P. M.; van Veggel, F. C. J. M.; Reinhoudt, D. N. *J. Org. Chem.* **1998**, *63*, 1299.
(32) Grootenhuis, P. D. J.; Kollman, P. A.; Groenen, L. C.; Reinhoudt, D. N.; van Hummel, G. J.; Ugozzoli, F.; Andreetti, G. D. *J. Am. Chem. Soc.* **1990**, *112*, 4165.
(33) Bernardino, R. J.; Costa Cabral, B. J. *J. Phys. Chem. A* **1999**, *103*, 9080.
(34) Hay, B. P.; Nicholas, J. B.; Feller, D. *J. Am. Chem. Soc.* **2000**, *122*, 10083.
(35) Suwattanamala, A.; Magalhaes, A. L.; Gomes, J. *Chem. Phys. Lett.* **2004**, 385, 368.
(36) Schatz, J.; Backes, A. C.; Siehl, H. U. *Perkin Trans. 2* **2000**, 609.
(37) Katsyuba, S. A.; Schmutzler, R.; Hohm, U.; Kunze, C. *J. Mol. Struct.* **2002**, *610*, 113.
(38) Katsyuba, S. A.; Chernova, A.; Schmutzler, R. *Org. Biomol. Chem.* **2003**, *1*, 714.
(39) Aleman, C.; den Otter, W. K.; Tolpekina, T. V.; Briels, W. J. *J. Org. Chem.* **2004**, *69*, 951.
(40) Yuan, H. S.; Zhang, Y.; Hou, Y. J.; Zhang, X. Y.; Yang, X. Z.; Huang, Z. T. *Tetrahedron* **2000**, *56*, 9611.
(41) Otsuka, H.; Suzuki, Y.; Ikeda, A.; Araki, K.; Shinkai, S. *Tetrahedron* **1998**, *54*, 423.
(42) Oshima, T.; Inoue, K.; Uezu, K.; Goto, M. *Anal. Chim. Acta* **2004**, *509*, 137.
(43) Otsuka, H.; Shinkai, S. *Supramol. Sci.* **1996**, 3, 189.

(44) Frisch, M. J.; Trucks, G. W.; Schlegel, H. B.; Scuseria, G. E.; Robb, M. A.; Cheeseman, J. R.; Montgomery, J. A., Jr.; Vreven, T.; Kudin, K. N.; Burant, J. C.; Millam, J. M.; Iyengar, S. S.; Tomasi, J.; Barone, V.; Mennucci, B.; Cossi, M.; Scalmani, G.; Rega, N.; Petersson, G. A.; Nakatsuji, H.; Hada, M.; Ehara, M.; Toyota, K.; Fukuda, R.; Hasegawa, J.; Ishida, M.; Nakajima, T.; Honda, Y.; Kitao, O.; Nakai, H.; Klene, M.; Li, X.; Knox, J. E.; Hratchian, H. P.; Cross, J. B.; Bakken, V.; Adamo, C.; Jaramillo, J.; Gomperts, R.; Stratmann, R. E.; Yazyev, O.; Austin, A. J.; Cammi, R.; Pomelli, C.; Ochterski, J. W.; Ayala, P. Y.; Morokuma, K.; Voth, G. A.; Salvador, P.; Dannenberg, J. J.; Zakrzewski, V. G.; Dapprich, S.; Daniels, A. D.; Strain, M. C.; Farkas, O.; Malick, D. K.; Rabuck, A. D.; Raghavachari, K.; Foresman, J. B.; Ortiz, J. V.; Cui, Q.; Baboul, A. G.; Clifford, S.; Cioslowski, J.; Stefanov, B. B.; Liu, G.; Liashenko, A.; Piskorz, P.; Komaromi, I.; Martin, R. L.; Fox, D. J.; Keith, T.; Al-Laham, M. A.; Peng, C. Y.; Nanayakkara, A.; Challacombe, M.; Gill, P. M. W.; Johnson, B.; Chen, W.; Wong, M. W.; Gonzalez, C.; Pople, J. A. *Gaussian 03*, revision B.05; Gaussian, Inc.: Pittsburgh, PA, 2004.

(45) Adamo, C.; Barone, V. *J. Chem. Phys.* **1999**, *110*, 6158.

(46) Perdew, J. P.; Burke, K.; Ernzerhof, M. *Phys. Rev. Lett*. **1996**, 77, 3865.

(47) Adamo, C.; Barone, V. *Chem. Phys. Lett*. **1997**, *274*, 242.

(48) Krishnan, R.; Binkley, J. S.; Seeger, R.; Pople, J. A. *J. Chem. Phys*. **1980**, *72*, 650.

(49) Cheeseman, J. R.; Frisch, M. J.; Trucks, G. W.; Keith, T. A. *J. Chem. Phys.* **1996**, *104*, 5497.

(50) Tomasi, J.; Persico, M. *Chem. Rev.* **1994**, *94*, 2027.

(51) Barone, V.; Cossi, M.; Tomasi, J. *J. Chem. Phys*. **1997**, *107*, *3210*.

(52) Barone, V.; Cossi, M. *J. Phys. Chem. A* **1998**, *102*, 1995.

(53) Magrans, J. O.; de Mendoza, J.; Pons, M.; Prados, P. *J. Org. Chem.* **1997,** *62* (13), 4518.

(54) Stewart, J. P. In *Reviews in Computational Chemistry*; Lipkowitz, K. B., Boyd, D. B., Eds.; VCH Publishers: New York, 1991; Vol. 3.

(55) Bernal-Uruchurtu, M. I., Martins-Costa, M. T. C.; Millot, C.; Ruiz-López, M. F. *J. Comput. Chem.* **2000**, *21*, 572

(56) Dado, G. P.; Gellman, S. H. *J. Am. Chem. Soc*. **1992**, *114*, 3138

(57) Zhao, Y.; Truhlar, D. G. *J. Chem. Theory Comput.* **2005**, *1*, 415

(58) Jabin, J. I.; Reinaud, O. *J. Org. Chem.* **2003**, *68*, 3416.

(59) Wiberg, K. B. *J. Comput. Chem.* **1999**, *20*, 1299.